

# Field distortion by a single cavity in HVDC XLPE cable under steady state

ISSN 2397-7264


Received on 5th May 2016

Revised on 11th July 2016

Accepted on 23rd July 2016

doi: 10.1049/hve.2016.0013

www.ietdl.org

Miao He , George Chen, Paul L. Lewin

Faculty of Physics and Applied Science, School of Electronic and Computer Science, University of Southampton, Southampton, UK

✉ E-mail: mh3e12@soton.ac.uk

**Abstract:** Electric field distribution in high voltage direct current (HVDC) cross-linked polyethylene (XLPE) cable at steady state is researched in this study. Under the condition that no cavity exists, equations describing the critical temperature difference for field reversal, and electric field distribution at steady state are proposed. When the cable with cavity is studied via the finite element analysis method, 2D and 3D model can be two possible choices. The comparison between these two models provides the reference for model selection so that the problem can be solved correctly. To study field enhancement by a single air-filled cavity at steady state, some possibly influenced factors are considered, including the cavity location, cavity size, cavity shape, temperature difference and material type. The equation describing field enhancement is given in the study.

## 1 Introduction

Development of high voltage direct current (HVDC) technology experiences a long history. The first HVDC underground cable was established in the year 1882 to transmit energy to New York City [1]. Another early operation is that HVDC cable connected Gotland Island to the mainland of Sweden with the power rating at 20 MW in 1954 [2–4]. The development of HVDC cable technology is fast in terms of capacity and voltage. Cable voltage can be as high as 600 kV [5], and the power rating can be as high as 1500 MW [6].

Compared with high voltage alternating current (HVAC) transmission system, HVDC system is with easier grid connection (without considering the network synchronicity) [7, 8] and fast and fully controllable power flow [8, 9]. Another significant advantage of HVDC system is that it is more applicable in long-distance power transmission: it is with lower power loss than HVAC transmission system for the same power capacity [7], and long-distance transmission can possibly compensate the weakness that HVDC system with higher capital expense due to the construction of converters and inverters [1, 6]. In 2007, the European Commission set up a European climate and energy 20/20/20 target towards the year of 2020 in helping reduce the greenhouse gas emissions, reducing the traditional energy consumption and enhancing energy efficiency [5, 10]. HVDC cable is also suitable for transmission of the offshore wind power to the mainland [7], and therefore it helps meet the European climate and energy goal.

Insulation materials used in HVDC cable are mass-impregnated and cross-linked polyethylene (XLPE). HVDC XLPE is with high volume resistivity, high dielectric strength, long DC lifetime and low space charge accumulation [11], and the permissible conductor temperature of XLPE cable is higher than the paper insulated cable [11]. The maximum operating temperature can be as high as 90°C [12].

Defects and cavities can be present in polymeric cable insulation. There are two ways through which cavities or defects appear inside the insulation. First, cavity or defect can possibly appear in the XLPE manufacture or fabrication process [12]. Second, new defects can possibly appear in operation. Under high field, which is defined as over 15 kV.mm<sup>-1</sup> for polyethylene [13], energy obtained by injected electrons from electric field exceeds the cohesive energy, and it is high therefore high enough in breaking the Van der Waal bonds [13,

14]. Accordingly, submicrocavities with the size determined by the maximum length of barrier width appear in the insulation [13, 14], and they can be experimentally detected. Due to aging, submicrocavities can possibly tend to coalesce to form cavities [13]. The presence of defects in XLPE cables can affect the electrical performance by disturbing the electric field distribution.

Local field distortion by a single spherical or ellipsoidal cavity has been investigated and published in several papers [15–18]. Under AC condition, the presence of cavity enhances the local field strength due to the difference in permittivity between air inside the cavity and the surrounding dielectric, and the relative permittivity of dielectric determines the enhancement percentage. However, not much work is published on the research in local field distortion by a single cavity in HVDC cable. Electrical conductivity is the key factor determining field distribution at steady state, and it is worth discussing the possibility that field enhancement at DC voltage can be expressed in a similar form to that at AC voltage with the relative permittivity replaced by the electrical conductivity. Electric field around a cavity can be numerically computed.

In the early research, simplified 2D model was often used to investigate the influence of the cavities [15–18]. In reality, the single spherical cavity described in 2D model simulates a cylindrical cavity with its axis parallel to the cable axis and having the same length as the cable, which does not exist in the real cables. Compared with 2D model, 3D model reflects the practical condition, and the cavity with different shapes, i.e. spherical or ellipsoidal, can be simulated by 3D model, leading to better accuracy in describing the electric field.

The finite element analysis (FEA) method is the tool in helping analyse the electric field distribution across the insulation or at the cavity. A popular software, COMSOL is used to build the model and calculate the electric distribution in HVDC XLPE cable at the steady state. Data is extracted from COMSOL and processed via the MATLAB to increase the flexibility in data analysis.

The aim of this paper is to study the electric field distribution of HVDC XLPE cable and the local field enhancement at steady state in the presence of a single air-filled cavity. In Section 2, equations describing field distribution across the insulation are introduced. In Section 3, the effect of cavity appearance on local field and the difference between 2D and 3D model are described. Parameters describing the cable size and material properties are listed in Section 4. Simulation results and their implication are given in Section 5.

## 2 Equation deductions

Equations describing electric field distribution of HVDC XLPE cable without cavity at steady state are proposed in this section. The assumptions for equation deduction are that, first, HVDC XLPE cable has been operated under the steady state for long period of time. Second, the dielectric material is isotropic. Third, no defect or cavity exists in the insulation layer.

The XLPE cable is cut into a small ‘cheese-like’ piece (shown in Fig. 1). The value of the central angle,  $\theta$ , is extremely small, and two points ( $x_1$  and  $x_2$ ) are extremely close. Under the steady state, it can be believed that leakage current flowing through this piece is all in the direction in parallel to the line crossing  $x_1$  and  $x_2$ .

$$I_1 = I_2 \quad (1)$$

$$E_1 \sigma_1 \theta x_1 dy = E_2 \sigma_2 \theta x_2 dy \quad (2)$$

where  $I_1$  and  $I_2$  are current through  $x_1$  and  $x_2$ .  $E_1$  and  $\sigma_1$  are field strength and electrical conductivity at  $x_1$ .  $E_2$  and  $\sigma_2$  are field strength and electrical conductivity at  $x_2$ .  $x_1$  and  $x_2$  are the distance of  $x_1$  and  $x_2$  to the cable centre.  $dy$  is the thickness of the selected piece. According to (2), the product value of local field, electrical conductivity and the distance to the cable centre is a constant across the insulation under each specific cable geometry, electrical condition and thermal condition.

$$E \sigma x = k \quad (3)$$

$E$  and  $\sigma$  represent the local field and electrical conductivity,  $x$  is the distance to the cable centre, and  $k$  is a product value. The expression is available for  $R_i \leq x \leq R_o$ , and it agrees with the conclusions given in [19]. Equation (3) is a basic equation for the conclusions obtained in this paper. The critical temperature difference across insulation layer for field reversal and electric field distribution will be given in next part.

### 2.1 Critical thermal condition for field reversal

Electrical conductivity of the insulation materials is a function of both temperature and electric field. A common equation in describing the electrical conductivity in DC cable indicates that electrical conductivity depends on both temperature and electric field exponentially [19]. In the recent research, however, an alternative relationship is much more preferred by researchers in describing the HVDC XLPE cable [19, 20]

$$\sigma(E, T) = A \exp\left(\frac{-\varphi q}{k_b T}\right) \frac{\sinh(B|E|)}{E} \quad (4)$$

at DC voltage.  $A$  and  $B$  are constants in the unit of  $A \cdot m^{-2}$  and  $m \cdot V^{-1}$ ,  $\varphi$  is the thermal activation energy in eV, and  $q$  is the elementary charge.  $T$  and  $E$  are the local temperature (K) and field strength ( $V \cdot m^{-1}$ ). Electrical conductivity is a field and temperature dependent parameter, and field reversal can possibly happen: the

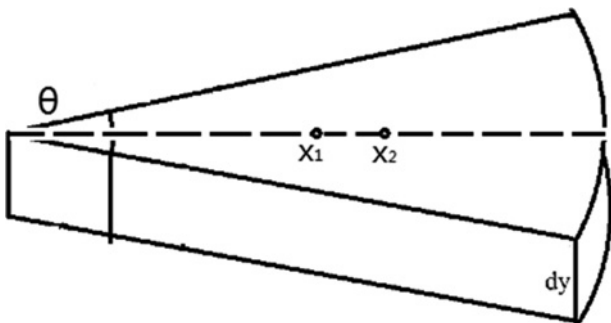


Fig. 1 ‘Cheese-like’ piece of the HVDC XLPE cable

insulation closer to the conductor has higher field strength are seen at low temperature difference ( $\Delta T$ ) across cable, and it generally happens at the early stage that cable is put into operation. Length of the stage depends on the load value. Current through the conductor keeps heating conductor. If  $\Delta T$  value exceeds a critical level, which is defined as  $\Delta T_{cri}$ , the phenomenon ‘field reversal’ appears at the steady state, and dielectric closer to the conductor is with lower field strength.

Equation (3) can be developed into the form that

$$A \exp\left(\frac{-\varphi q}{k_b T}\right) \sinh(B|E|) x = k \quad (5)$$

if (4) is introduced. Considering the innermost and outermost insulation layer, we have

$$A \exp\left(\frac{-\varphi q}{k_b T_i}\right) \sinh(B|E_i|) R_i = A \exp\left(\frac{-\varphi q}{k_b T_o}\right) \sinh(B|E_o|) R_o \quad (6)$$

$i$  and  $o$  in the script mean the innermost and outermost insulation layer. It is stated that field is a monotonous function to the radius [20]. Therefore,  $E_i$  equals to  $E_o$  under the critical thermal condition that  $\Delta T = \Delta T_{cri}$

$$-\frac{\varphi q}{k_b T_i} + \ln R_i = -\frac{\varphi q}{k_b T_o} + \ln R_o \quad (7)$$

$$M = \frac{\varphi q}{k_b} \quad (8)$$

$$\Delta T_{cri} = T_i - T_o = \frac{T_o^2 \ln(R_o/R_i)}{M - T_o \ln(R_o/R_i)} \quad (9)$$

$M$  is a parameter in simplifying the expression. The critical temperature difference level is determined by the ratio of outer radius to the inner radius, outer layer temperature, and the material properties. Across the cable service time, insulation gradually degrades due to field strength and temperature, and the critical value can possibly change.

### 2.2 Temperature distribution across cable

Though the paper focuses on electric field, it is essential to calculate the temperature distribution at DC voltage as it determines the electrical conductivity [20]. It has been noted that in mass-impregnated cable, electric field at the middle of cable insulation tends to keep more or less constant at the steady state [21–23]. The measurement results in [21] indicate that under the voltage lower than the maximum thermal voltage, the increase rate of field at the middle of insulation in XLPE cable nearly equals to the increase rate of applied voltage. Therefore, the point that electric field at the middle of cable,  $E_c$ , keeps nearly constant is available for the XLPE cable as well.

$$E_c = \frac{U}{R_o - R_i} \quad (10)$$

$U$  is the magnitude of externally applied voltage. Equation (5) is further developed into

$$A \exp\left(\frac{-\varphi q}{k_b T_c}\right) \sinh(B|E_c|) R_c = A \exp\left(\frac{-\varphi q}{k_b T_o}\right) \sinh(B|E_o|) R_o \quad (11)$$

$c$  in the script means the middle of the insulation. Under the specific

condition that  $\Delta T = \Delta T_{\text{cri}}$ ,  $E_c = E_o$ .

$$-\frac{\varphi q}{k_b T_c} + \ln R_c = -\frac{\varphi q}{k_b T_o} + \ln R_o \quad (12)$$

$$T_c = \frac{1}{(1/T_o) - ((\ln R_o - \ln R_c)/M)} \quad (13)$$

Equation (13) is only meaningful when field reversal is close to happen. To propose a general temperature distribution equation, (13) is rewritten as

$$T_x = \frac{1}{(1/T_o) - f((\ln R_o - \ln R_x)/M)} \quad (14)$$

where  $T_x$  is the temperature at  $R_x$  ( $R_i \leq R_x \leq R_o$ ), and  $f$  is a modification factor. For  $R_x = R_i$

$$T_i = \frac{1}{(1/T_o) - f((\ln R_o - \ln R_i)/M)} \quad (15)$$

$$f = \frac{M \Delta T}{T_i T_o (\ln R_o - \ln R_i)} \quad (16)$$

Therefore

$$T_x = \frac{T_o * (T_o + \Delta T)}{T_o + \Delta T * (\ln R_x - \ln R_i / \ln R_o - \ln R_i)} \quad (17)$$

No material property related parameters appear in the equation, and temperature distribution is determined by the outer layer temperature, temperature difference across the cable, cable geometry and the distance to cable centre.

### 2.3 $k$ value calculation

Equation (3) is a basic equation in drawing important conclusions in this paper, and it is useful to find a way in calculating the value of  $k$ . Having known the temperature distribution equation, (3) is

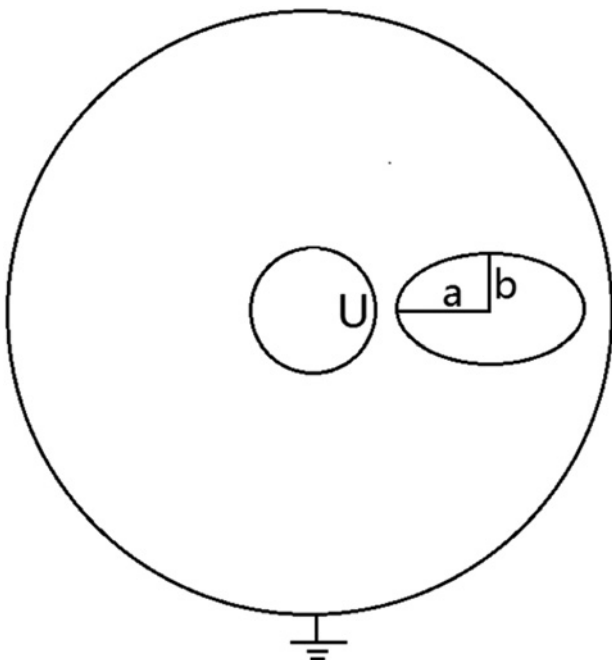


Fig. 2 Shape of cavity

Table 1 Parameters applied in simulation [6, 20, 28]

Name	Value	Description
$U$	150,000	applied voltage, unit: V
$R_i$	29.854	inner radius, unit: mm
$R_o$	63	outer radius, unit: mm
$l$	0.5	cable length, unit: m
$T_o$	301.15	outer temperature, unit: K
$\Delta T$	3; 7; 12; 20	temperature difference across cable, unit: K
$R_c$	0.5, 1, 1.5	radius of the spherical cavity, unit: mm
$A$	3.2781	constant of 'good' material, unit: $A \cdot m^{-2}$
	$3.6782 \times 10^7$	constant of 'bad' material, unit: $A \cdot m^{-2}$
$B$	$2.7756 \times 10^{-7}$	constant of 'good' material, unit: $m \cdot V^{-1}$
	$1.086 \times 10^{-7}$	constant of 'good' material, unit: $m \cdot V^{-1}$
$\varphi$	0.56	thermal activation energy of 'good' material, unit: eV
	0.98	thermal activation energy of 'bad' material, unit: eV
$\sigma_{\text{air}}$	$1 \times 10^{-16}$	electrical conductivity of air when no PD occurs, unit: $S \cdot m^{-1}$
$\epsilon_r$	2.3	relative permittivity of XLPE

developed as

$$k = A \exp\left(\frac{-\varphi q}{k_b T_c}\right) \sinh(B|E_c|) R_c \quad (18)$$

when  $x = R_c$ . Temperature at the middle of insulation can be calculated according to (17). Under the constant DC applied voltage, value of  $k$  is determined by the thermal condition ( $T_c$ ) and the material properties ( $\varphi$ ).

### 2.4 Field distribution across cable

Under the known value of  $T_o$  and  $\Delta T$ , electric field at any point on the insulation layer can be obtained via

$$\exp\left(\frac{-\varphi q}{k_b T_x}\right) \sinh(B|E_x|) = \frac{k}{AR_x} \quad (19)$$

$$P = \ln \frac{2k}{AR_x} + \frac{M}{T_x} \quad (20)$$

$$E_x = \frac{1}{B} \ln \frac{\exp(P) + \sqrt{\exp(2P) + 4}}{2} \quad (21)$$

## 3 Cavity distortion on local field

The electric field distribution when no cavity exists in the insulation has been described in the above section. In practice, it is possible that cavity exists inside the insulation. The appearance of cavity can not only influence the field inside cavity, but also distort field surrounding the cavity. The previous research as [15–18] have shown that the air-filled cavity enhances the local field as the relative permittivity of air is lower than the XLPE.

Under AC voltage, field across insulation is capacitively graded, and relative permittivity is a key factor in determining field distribution. Field enhancement under the condition by a single air-filled cavity can be expressed by the following equation [24]

$$\eta_{\text{AC}} = \frac{K \epsilon_r}{\epsilon_0 + (K - 1) \epsilon_r} \quad (22)$$

$K$  is a coefficient, and the value is determined by the axis ratio of cavity,  $a/b$  (as shown in Fig. 2) [24, 25]. If  $a/b$  equals to one, it is a spherical cavity. If  $a/b$  is not unit, it is an ellipsoidal cavity.  $\epsilon_r$  and  $\epsilon_0$  are the relative permittivity of XLPE and vacuum permittivity.

Electric field tends to be resistively graded in HVDC cable at steady state, and electrical conductivity is an important parameter that determines electric field distribution. In describing field enhancement by a single air-filled cavity in HVDC XLPE cable at

steady state, a speculation is that the relative permittivity in (22) can be straightforwardly replaced by the electrical conductivity

$$\eta_{DC} = \frac{K\sigma_{XLPE}}{\sigma_{air} + (K-1)\sigma_{XLPE}} \quad (23)$$

$\sigma_{XLPE}$  and  $\sigma_{air}$  are the electrical conductivity of XLPE at the steady state and air without the occurrence of discharge. Availability of the speculation is to be proved in Section 5.

#### 4 Parameters setting and data selection

Parameters used in the FEA method are listed in Table 1. Temperature of the cable outer layer is set to be constant in simplifying the analysis. In [26, 27], conductivity of air is calculated as

$$\sigma_{air} = \sigma_{max} \left\{ 1 - \exp \left[ - \left( \left| \frac{U}{U_{inc}} \right| + \left| \frac{I}{I_{crit}} \right| \right) \right] \right\} \quad \text{with PD} \quad (24)$$

$$\sigma_{air} = 0 \quad \text{no PD} \quad (25)$$

$\sigma_{max}$  is the maximum conductivity during discharge,  $I_{crit}$  is the critical current starting electron avalanche,  $U$  is the voltage across cavity, and  $U_{inc}$  is the inception voltage. However, if the conductivity is setting according to (25), the influence of  $\sigma_{XLPE}$ , i.e. thermal condition and location at insulation, cannot be reflected in HVDC cable at steady state according to (23). In [28], air-conductivity can be with a level in the order of  $10^{-6} \text{ S.m}^{-1}$  at 293.15 K. Therefore, the air conductivity is set as  $1 \times 10^{-16} \text{ S.m}^{-1}$ .

Values of  $A$ ,  $B$  and  $\varphi$  depend on the condition of material. According to Boggs *et al.* [20], there are two groups of value. The ones defined as 'good' describe the properties of XLPE at the start stage of lifetime, and the ones defined as 'bad' describe properties of XLPE after long-term degradation. Research on the influence of material properties on electric field distribution can be realised via using the corresponding data.

Value of  $\Delta T_{crit}$  calculated according to (9) differs depending on the conditions of material, being 10.81 and 6.08 K for 'good' and 'bad' material, respectively. In studying the situation before and after field reversal happens, four levels of  $\Delta T$  are used in the paper. For 'good' material, for example, 3 and 7 K is for the condition that field reversal does not occur, and 12 and 20 K are for the condition that field reversal appears. To study the influence of cavity size three cavity radius values have been used in analysis.

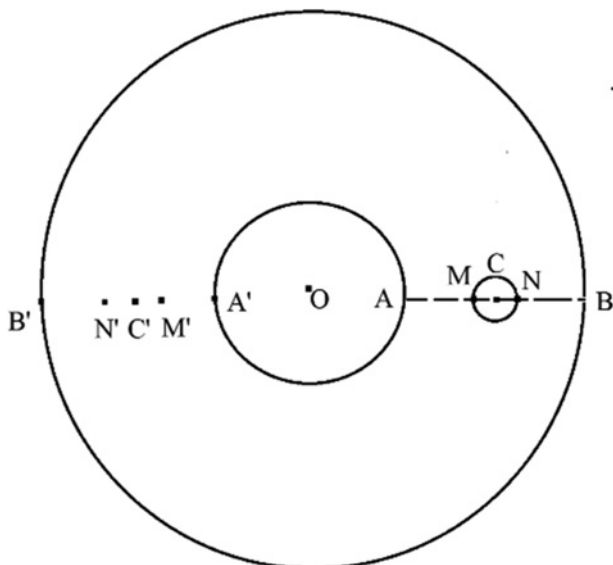


Fig. 3 Data selection method indication

Fig. 3 indicates the cross-section of the cable through the cavity centre. The distance of cavity centre (C) to the cable centre (O) is expressed as

$$X = R_i + a(R_o - R_i) \quad (26)$$

and  $a$  is the distance ratio indicating the distance of cavity centre to the cavity centre. Lower value of  $a$  means that the cavity is closer to the cable centre. The equation is meaningful when  $(R_i + R_c) < X < (R_o - R_c)$ . A and B is on the innermost layer and outermost layer of insulation, and points O, A, C and B are on the same line. M N are two points shared by the cavity and line AB. Points A', B' and C' are the mirror points of A, B and C.

Lines AB and A'B' are both uniformly divided into 500 small section with the same length. Electric field, electrical conductivity and the distance to cable centre of each small section are recorded. Values on AB are to describe the characteristics across insulation after cavity appears, while those on A'B' are to reflect characteristics across insulation before cavity appears. Lines MN and M'N' are uniformly divided into 100 small section, and field of each section is recorded.

#### 5 Results

On the basis of equations describing the field distribution across HVDC XLPE cable at steady state without cavity, and field enhancement by a single cavity at steady state, simulations are to be carried out in this section. The influence of cavity size, cavity location, cavity shape, temperature difference, and material properties are considered.

##### 5.1 Model reliability prove

Under AC voltage, field inside and outside the spherical cavity can be calculated as [29]

$$E = E_0 \left( \frac{3\varepsilon_r}{\varepsilon_0 + 2\varepsilon_r} \right) (-i_r \cos \theta - i_\theta \sin \theta) \quad (27)$$

$$E = E_0 \left( i_r \left( -1 - \left( \frac{\varepsilon_0 - \varepsilon_r}{\varepsilon_0 + 2\varepsilon_r} \right) \frac{2R_c^3}{r^3} \right) \cos \theta + i_\theta \left( 1 - \left( \frac{\varepsilon_0 - \varepsilon_r}{\varepsilon_0 + 2\varepsilon_r} \right) \frac{R_c^3}{r^3} \right) \sin \theta \right) \quad (28)$$

$E_0$  is the field when no cavity appears, and  $r$  is the distance from cavity centre.  $i_r$  and  $i_\theta$  are unit vectors of insulation coordinate

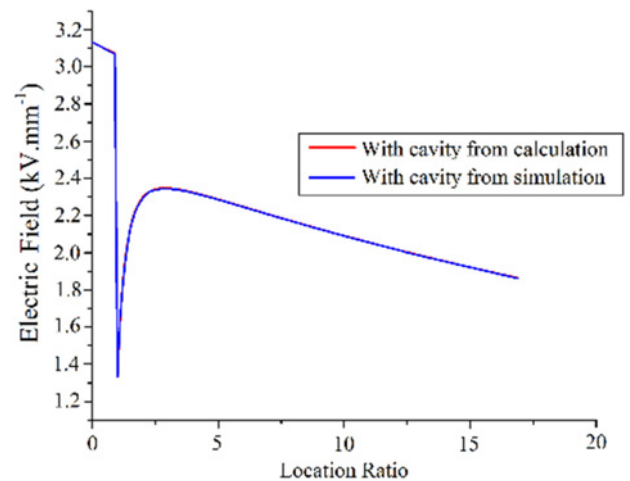
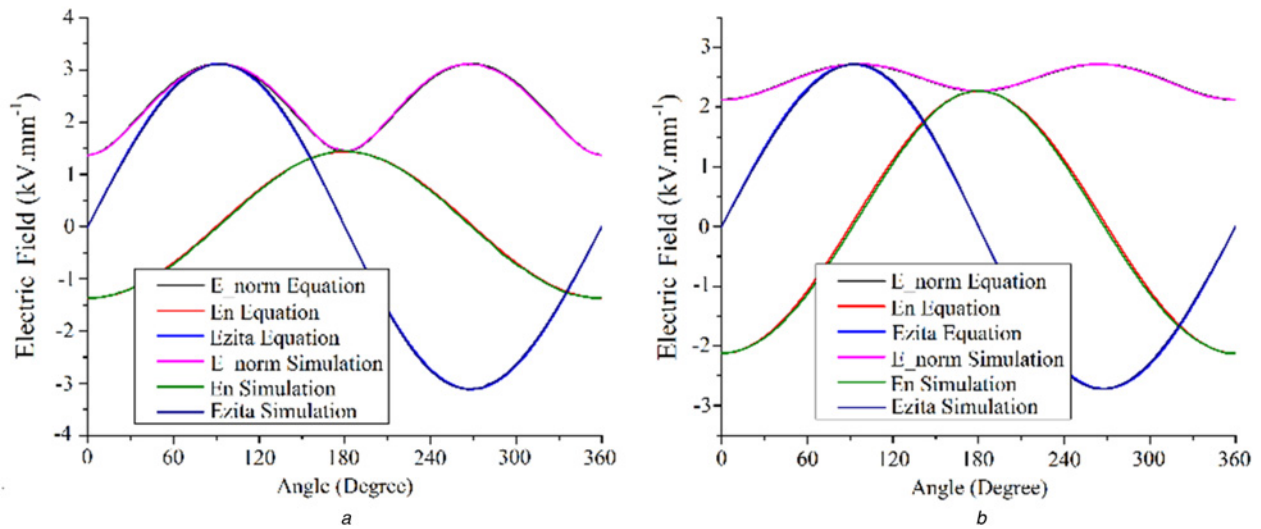


Fig. 4 Comparison between calculation and simulation results in field distribution across cable at  $t = 0.002 \text{ s}$  (1/10 cycle time)



**Fig. 5** Comparison between calculation and simulation results in field distribution

a At the cavity surface at  $t=0.002$  s (1/10 cycle time,  $1.01R_c$  to cavity centre)  
b Surrounding the cavity at  $t=0.002$  s (1/10 cycle time,  $1.5R_c$  to cavity centre)

system.  $\theta$  is the angle value determining the location. Equation (27) is available for  $0 \leq r < R_c$ , and (28) is meaningful for  $r > R_c$ .

The simulation results are given in Figs. 4 and 5. The maximum magnitude is 150 kV, voltage frequency is 50 Hz, and cable geometry follows the data in Table 1. It can be seen that simulation results agree with calculation results for crossing the insulation (Fig. 4) and surrounding the cavity (Fig. 5). Therefore, simulation results are reliable.

## 5.2 $\Delta T_{cri}$ value calculation

Reliability in calculating the critical temperature difference value using (9) is shown in Fig. 6. The gap between the calculation results and the simulation results is negligible (never higher than 0.1 K). Therefore, (9) is reasonable.

The critical value from ‘good’ material is higher than that of ‘bad’ material. Insulation keeps degrading across the cable operation, and the material goes from ‘good’ to ‘bad’. Therefore, field reversal can possibly happen though cable has been at steady state for long. For example, under the data given in Table 1, if the temperature difference keeps at 9 K, field is higher at the region closer to conductor at the start stage as the insulation is good ( $\Delta T_{cri} = 10.81$  K). The critical value keeps decreasing due to degradation, and field reversal can possibly occur (for ‘bad’ material,  $\Delta T_{cri} = 6.08$  K).

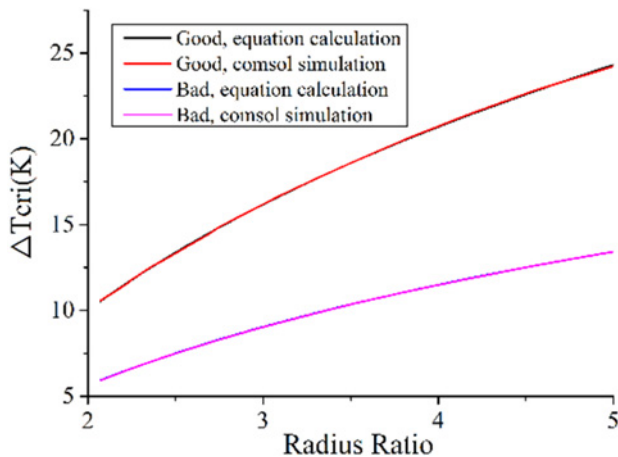


**Fig. 6** Comparison between the calculation and simulation results in  $\Delta T_{cri}$  across various  $R_o/R_i$  value

## 5.3 Field distribution calculation

Fig. 7 shows the availability in calculating field distribution using (21). Three levels of temperature difference are used in considering the influence of field reversal occurrence. It has been seen that the field distribution follows (21) with a small gap. The reason can be that (21) is proposed assuming that electric field strength at the middle of insulation is constant [21–23], while electric field strength at the middle layer fluctuates slightly in practice.

## 5.4 Field enhancement by cavity

As shown in Fig. 3, the average electric field strength inside cavity is calculated via adding field on MN over the total number of division. Similarly, the average field of  $M'N'$  is set as the reference field in calculating the field enhancement. Equation (27) indicates electric field inside cavity under AC voltage is uniformly distributed. Similar feature has been observed under DC voltage (as shown in Fig. 8). The gap between the maximum and minimum strength is little (not higher than 5% and  $0.35 \text{ kV}\cdot\text{mm}^{-1}$ ). Therefore, the average electric field strength inside the cavity is used in studying field enhancement by the cavity.

Appearance of cavity distorts the local field at the cavity. Local field distortion, or field enhancement, is calculated as

$$\eta = \frac{E_{cav.ave}}{E_{cav'.ave}} \times 100\% \quad (29)$$

$E_{cav.ave}$  is the average field along MN, while  $E_{cav'.ave}$  is the average strength along  $M'N'$ . As discussed in Section 1, simulation results from 2D and 3D models should be different in field enhancement calculation. Fig. 9 shows the model comparison in local electric field strength at the spherical cavity. Results from 2D model is higher than those from 3D model. Data on field strength and the field enhancement value from 2D and 3D model is listed in Table 2: field enhancement value from 2D model can be nearly 30% higher than that from 3D model.

Moreover, in the region far from the cavity centre, for example, 5 times cavity radius away from the cavity, electric field results from 2D and 3D model equal. The reason is that the influence of cavity on the electric field is a local effect, and therefore the influence of cavity in the region far from the cavity is little. Accordingly, field enhancement by the single air-field is researched via the 3D model.

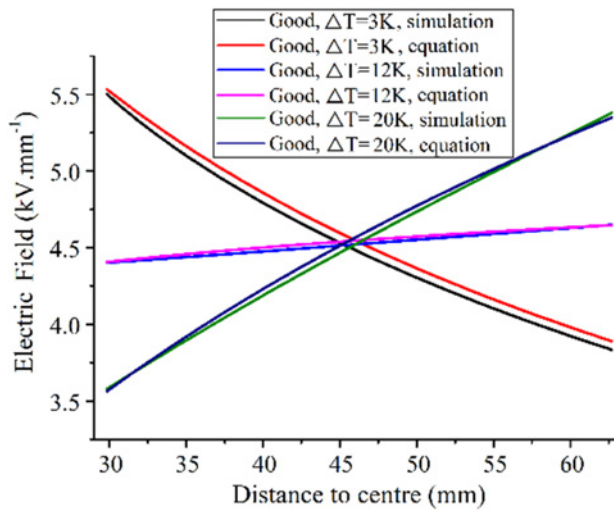


**Fig. 7** Comparison between the calculation and simulation results in electric field distribution across insulation under various temperature difference values

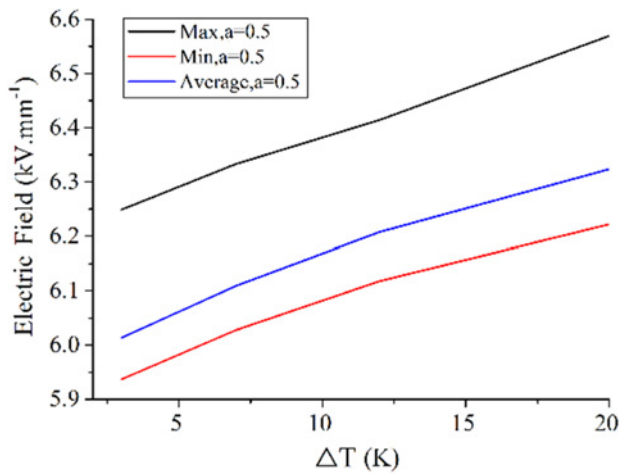


**Fig. 8** Maximum, minimum and average field strength inside cavity in HVDC cable ( $a = 0.5$ ,  $R_c = 1$  mm)

The relationship between the field enhancement and the cavity size and location under various thermal conditions is illustrated in Fig. 10. Field enhancement is independent of cavity size within

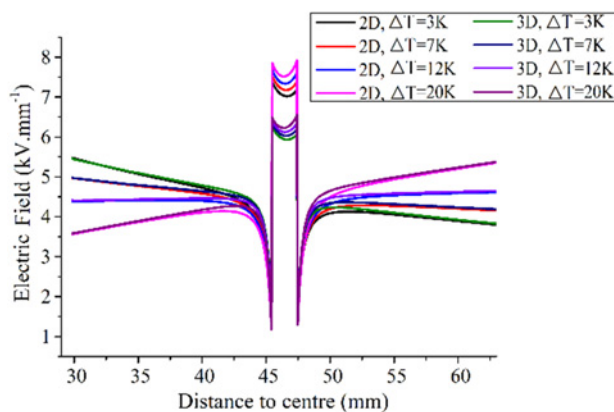


**Fig. 9** 2D and 3D model comparison on electric field distribution across cable when a single spherical cavity locates at the middle of insulation under different temperature difference

**Table 2** Electric field and field enhancement comparison

$\Delta T$ (K)	$E$ , $\text{kV}\cdot\text{mm}^{-1}$		$\eta$ , %	
	2D model	3D model	2D model	3D model
3	7.11	6.01	159.3134	134.72
7	7.27	6.11	161.7284	135.91
12	7.43	6.21	164.425	137.22
20	7.64	6.32	168.0488	139.14

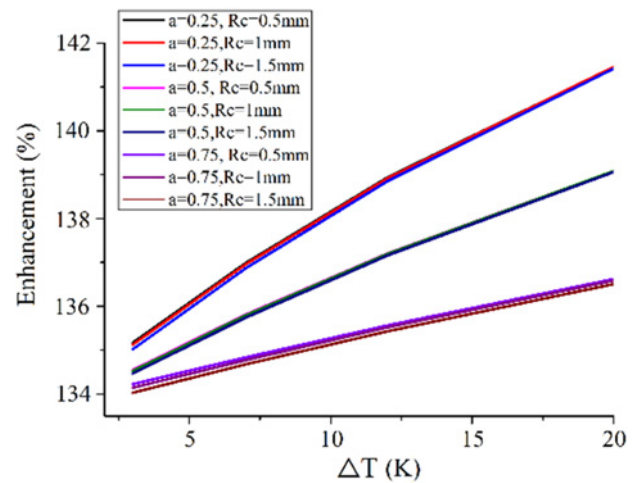


**Fig. 10** Field enhancement under various temperature difference for a single spherical cavity with different size and/or located at different places at the insulation layer

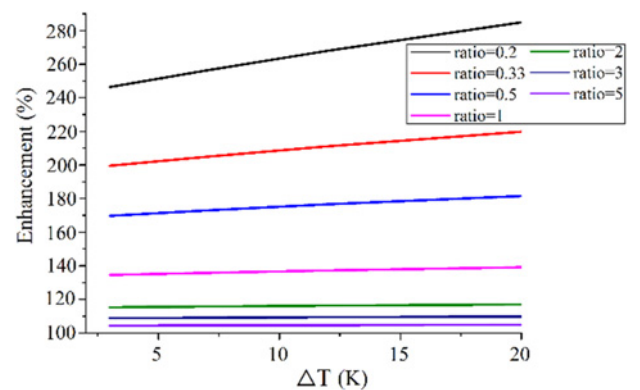


**Fig. 11** Relationship between enhancement by a single ellipsoidal cavity and the ratio under various temperature difference

the size range studied in this paper, but it varies with the cavity location. The reason is that electrical conductivity of surrounding XLPE,  $\sigma_{\text{XLPE}}$ , depends on temperature and electric field strength. At the same place on line M'N' in Fig. 3, electrical conductivity equals even though cavity size varies. Therefore, cavity size is not

**Table 3** Relationship between  $K$  and axis ratio [25]

Axis ratio, $a/b$	$K$
0.2	1.3325
0.33	1.5738
0.5	1.8968
1	3
2	5.7616
3	9.313
5	17.914

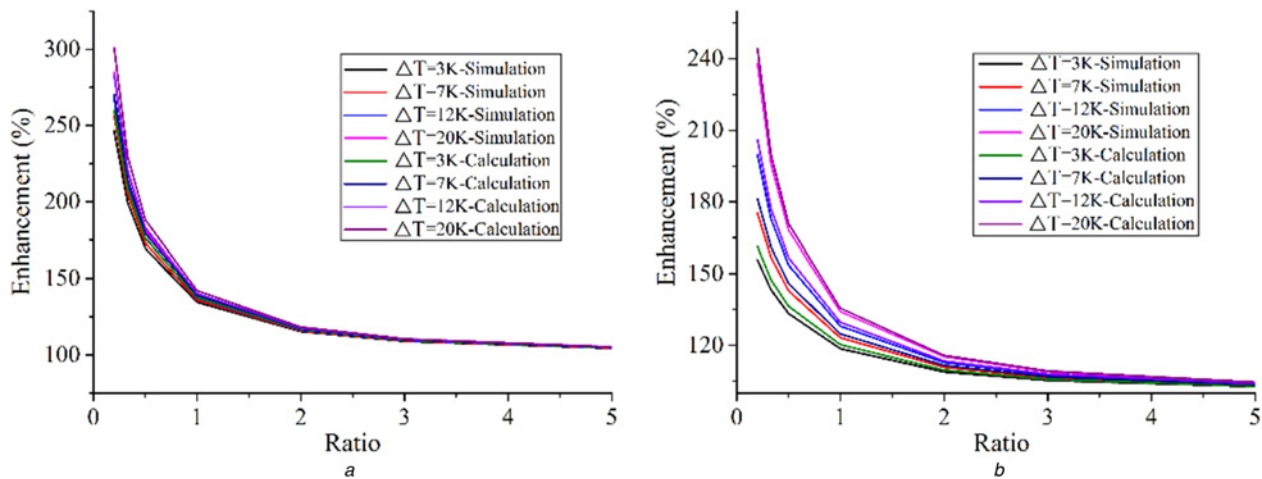


**Fig. 12** Comparison between the field enhancement by air-filled cavity from modelling and that from equation under different axis ratio and temperature difference

a In 'good' material  
b In 'bad' material

a key factor in field enhancement, while cavity location is important in HVDC cable under steady state.

Fig. 11 indicates the relationship between the field enhancement and the cavity shape. The cavity is placed at the middle of insulation. Though the axis ratio,  $a/b$ , varies, volume of the cavity keeps constant, equalling to the volume of the spherical cavity with 1 mm cavity radius. Location variation and cavity size are not considered in the cavity shape analysis as they have been demonstrated in Fig. 11. It shows that the cavity shape is a key factor in determining the field enhancement. The reason is that field enhancement value depends on the value of  $K$  (as given in (22)), which is determined by the axis ratio. The relationship between  $K$  and  $a/b$  is listed in Table 3.

According to the data listed in Table 3, the comparison between calculated field enhancement value via (23) and simulation results is illustrated in Fig. 12a. The difference between the simulation and calculation results is acceptably low, and therefore it can be believed that it is reliable in expressing the field enhancement by the single ellipsoidal cavity via (23). The importance of electrical conductivity in determining electric field at DC voltage is accordingly similar to that of relative permittivity in determining field at AC voltage. Fig. 12b shows the influence of material properties. Across various value of axis ratio level and temperature difference, conclusions drawn from 'good' material is suitable for the 'bad' material as well.

## 6 Conclusions

In this paper, field distribution in HVDC cable at steady state is researched. Under the condition that no cavity exists, the  $k$  value, product of electric field, electrical conductivity and distance from cable centre, is constant under each specific cable geometry, electrical condition and thermal condition. Equations describing the critical temperature difference for field reversal, and electric field distribution across insulation are deduced and proposed. All equations are proved to be practical and available via the agreement of calculated results to the FEA results.

2D and 3D models are different in reflecting the real condition. The comparison indicates that 3D model is the only choice if the researched is on the local field at the cavity. Field enhancement by cavity from 2D model can be nearly 30% higher than the practical condition which is obtained from 3D model.

At AC voltage, local electric field enhancement is determined by the relative permittivity and cavity shape. For HVDC cable steady state analysis, the FEA results indicate that the relative permittivity can be replaced with electrical conductivity in calculating the field

enhancement in calculating the field enhancement. This conclusion is available under the range of cavity size, cavity location, temperature difference across insulation, and material properties studied in the paper.

Research in this paper concentrates more on field inside the cavity. In future work, field surrounding the cavity will be researched, and the volume of region possibly distorted is to be studied. It reveals the local cavity distortion by cavity together with conclusions drawn in this paper.

## 7 References

- Mazzanti, G., Marzinotto, M.: 'Fundamentals of HVDC cable transmission, in extruded cables for high-voltage direct-current transmission: advances in research and development' (John Wiley & Sons, Inc., Hoboken, New Jersey, 2013)
- Long, W., Nilsson, S.: 'HVDC transmission: yesterday and today', *IEEE Power Energy Mag.*, 2007, 5, (2), pp. 22–31, doi: 10.1109/MPAE.2007.329175
- ABB's high voltage cable unit Sweden: 'HVDC light cables: Submarine and land power cables' (2006), p. 5
- Murata, Y., Sakamaki, M., Abe, K., et al.: 'Developments of high voltage DC-XLPE cable system', *SCI Tech. Rev.*, 2013, 76, pp. 55–62
- Ghorbani, H., Jeroense, M., Olsson, C.O., et al.: 'HVDC cable systems—highlighting extruded technology', *IEEE Trans. Power Deliv.*, 2014, 29, (1), pp. 414–421, doi: 10.1109/TPWRD.2013.2278717
- ABB's high voltage cable unit Sweden: 'HVDC Light Cables: Submarine and land power cables' (2006), p. 5
- Valenza, D., Cipollini, G.: 'HVDC submarine power cable systems—state of the art and future developments'. Int. Conf. on Energy Management and Power Delivery (EMPD), Milano, Italy, 1995, pp. 283–287
- Jeroense, M.: 'HVDC, the next generation of transmission highlights with focus on extruded cable systems'. Int. Symp. on Electrical Insulating Materials, 2008 (ISEIM 2008), Mie, 2008, pp. 10–15
- Chen, G., Hao, M., Xu, Z., et al.: 'Review of high voltage direct current cables', *CSEE J. Power Energy Syst.*, 2015, 1, (2), pp. 9–21, doi: 10.17775/CSEEJPES.2015.00015
- 'Limiting global climate change to 2 degrees Celsius the way ahead for 2020 and beyond. Communication from the commission to the council, the European Parliament, the Eur. Econ. and Social Committee and the Committee of the regions', <http://eurlex.europa.eu/LexUriServ/LexUriServ.do?uri=COM:2007:0002:FIN:EN:PDF>; HVDC cable systems—highlighting extruded technology, accessed January, 2007
- Igi, T., Murata, Y., Abe, K., et al.: 'Advanced HVDC XLPE cable and accessories'. 9th IET Int. Conf. on Advances in Power System Control, Operation and Management (APSCOM), Hong Kong, 2012, pp. 1–6
- Jain, V.K., Bajaj, A.: 'A textbook of design of electrical installations' (Laxmi Publications (P) LTD., 2004)
- Crine, J.P.: 'A molecular model to evaluate the impact of aging on space charges in polymer dielectrics', *IEEE Trans. Dielectr. Electr. Insul.*, 1997, 4, (5), pp. 487–495, doi: 10.1109/94.625641
- Crine, J.P., Pappal, J.L., Lessard, G.: 'A model of aging of dielectric extruded cables'. Proc. Third Int. Conf. on Conduction and Breakdown in Solid Dielectrics, Trondheim, 1989, pp. 347–351
- Lachini, S., Gholami, A., Mirzaie, M.: 'Determining electric field distribution in high voltage cable in presence of cavity'. 45th Int. Universities Power Engineering Conf. (UPEC), Cardiff, Wales, 2010, pp. 1–7

- 16 Blackburn, T. R., Phung, B.T., Zhang, H., *et al.*: 'Investigation of electric field distribution in power cables with voids'. Eighth Int. Conf. on Properties and applications of Dielectric Materials, Bali, 2006, pp. 637–640
- 17 Nosseir, A.r.: 'Calculation of discharge inception voltage due to the presence of voids in power cables', *IEEE Trans. Electr. Insul.*, 1979, **EI-14**, (2), pp. 117–120, doi: 10.1109/TEL.1979.298165
- 18 Cheng, F.C.: 'Insulation thickness determination of polymeric power cables', *IEEE Trans. Dielectr. Electr. Insul.*, 1994, **1**, (4), pp. 624–629, doi: 10.1109/94.311705
- 19 Mazzanti, G., Marzinotto, M.: 'Main principles of HVDC extruded cable design', in Mazzanti, G., Marzinotto, M. (Eds.): 'Extruded cables for high-voltage direct-current transmission: advances in research and development' (Wiley-IEEE Press, 2013), p. 384
- 20 Boggs, S., Damon, D.H., Hjerrild, J., *et al.*: 'Effect of insulation properties on the field grading of solid dielectric DC cable', *IEEE Trans. Power Deliv.*, 2001, **16**, (4), pp. 456–461, doi: 10.1109/61.956720
- 21 Fothergill, J.: 'The coming of age of HVDC extruded power cables'. Electrical Insulation Conf. (EIC), Philadelphia, PA, 2014, pp. 124–137
- 22 Huang, Z.Y., Pilgrim, J.A., Lewin, P.L., *et al.*: 'Thermal-electric rating method for mass-impregnated paper-insulated HVDC cable circuits', *IEEE Trans. Power Deliv.*, 2015, **30**, (1), pp. 437–444, doi: 10.1109/TPWRD.2014.2359772
- 23 Jeroense, M.J.P., Morshuis, P.H.F.: 'Electric fields in HVDC paper-insulated cables', *IEEE Trans. Dielectr. Electr. Insul.*, 1998, **5**, (2), pp. 225–236, doi: 10.1109/94.671940
- 24 Gutfleisch, F., Niemeyer, L.: 'Measurement and simulation of PD in epoxy voids', *IEEE Trans. Dielectr. Electr. Insul.*, 1995, **2**, (5), pp. 729–743, doi: 10.1109/94.469970
- 25 Crichton, G.C., Karlsson, P.W., Pedersen, A.: 'Partial discharges in ellipsoidal and spheroidal voids', *IEEE Trans. Electr. Insul.*, 1989, **24**, (2), pp. 335–342, doi: 10.1109/14.90292
- 26 Illias, H.A., Chen, G., Lewin, P.L.: 'Partial discharge modelling in a spherical cavity within a dielectric insulation material as a function of frequency'. Electrical Insulation Conf. (EIC), Montreal, QC, 2009, pp. 55–59
- 27 Forssen, C., Edin, H.: 'Modeling partial discharges in a cavity at different applied frequencies'. Electrical Insulation and Dielectric Phenomena (CEIDP), Vancouver, BC, 2007, pp. 132–135
- 28 Pawar, S.D., Murugavel, P., Lal, D.M.: 'Effect of relative humidity and sea level pressure on electrical conductivity of air over Indian Ocean', *J. Geophys. Res.*, 2009, **14**, p. D02205
- 29 Magid, L.M.: 'Electromagnetic fields, energy, and waves' (Wiley, New York, 1972)